ARTICLE IN PRESS

Available online at www.sciencedirect.com

SCIENCE DIRECT®

Journal of Computational Physics xxx (2005) xxx–xxx

JOURNAL OF COMPUTATIONAL PHYSICS

www.elsevier.com/locate/jcp

Short note

"Curl-q": A vorticity damping artificial viscosity for essentially irrotational Lagrangian hydrodynamics calculations

E.J. Caramana *, R. Loubère

CCS-2 and T-7, Los Alamos National Laboratory, MS-D413, Los Alamos, NM 87545, United States

Received 1 September 2005; received in revised form 8 November 2005; accepted 10 November 2005

1. Introduction

The bane of Lagrangian hydrodynamics calculations in multi-dimensions is the appearance of vorticity that causes tangling of the mesh and consequent run termination. This vorticity may be numerical or physical in origin, and is in addition to the spurious "hourglass" modes associated with quadrilateral or hexahedral zones that in pure form have both zero curl and divergence associated with their velocity field.

The purpose of this note is to introduce a form of vorticity damping, based on a previously published edge-centered artificial viscosity [1], that extends the runtime and range of calculations over which a pure Lagrangian code can compute. Since the explicit inclusion of an artificial viscosity into the fluid equations is often referred to as the "q term", we denote this new term as the "curl-q", because it is a function of the curl of the velocity field in a zone. It is formulated in the context of the "discrete, compatible formulation of Lagrangian hydrodynamics" [2,3]. This employs a staggered placement of variables in space (velocity and position at nodes, with density and stresses in zones), but a predictor/corrector time integration scheme so that all variables are known at the same time level, allowing total energy to be exactly conserved [2]. This new "curl-q" does not resolve shock waves and is always to be utilized with an artificial viscosity that performs this task. In order to set the stage for the introduction of the new curl-q force, the edge-centered artificial viscosity given in [1] is briefly reviewed in a slightly simplified form; after this the curl-q force is formulated as an analogy to this edge-centered artificial viscosity. Numerical results are given in both 2D and 3D that display its effectiveness. In particular, results are contrasted between this new term and a recently published tensor artificial viscosity [4]. It is shown that these two forms give quite similar results in 2D. We end with a brief discussion concerning the validity of the use of this type of numerical device.

In Fig. 1 is shown a quadrilateral zone with its defining points, $i = 1$–4, and associated median mesh vectors $\vec{S}_i$. These vectors point in the indicated direction and have a magnitude of the surface area that lies between their defining points in 2D or in 3D [2,5]. In terms of the median mesh vector $\vec{S}_1$, the force exerted by the edge-centered artificial viscosity between points "1" and "2" from zone "z" is given by

$$\vec{f}_{21}^{\,\mathrm{visc}} = c_1(1-\psi_{21})\rho_z(c_{s,z}+\Delta v_{21})[\Delta\vec{v}_{21}\cdot\vec{S}_1]\widehat{\Delta v_{21}}, \tag{1.1}$$

* Corresponding author. Tel.: +505 667 7779; fax: +505 667 3726.
E-mail addresses: ejc@lanl.gov (E.J. Caramana), loubere@lanl.gov (R. Loubère).

0021-9991/$ - see front matter. Published by Elsevier Inc.
doi:10.1016/j.jcp.2005.11.018

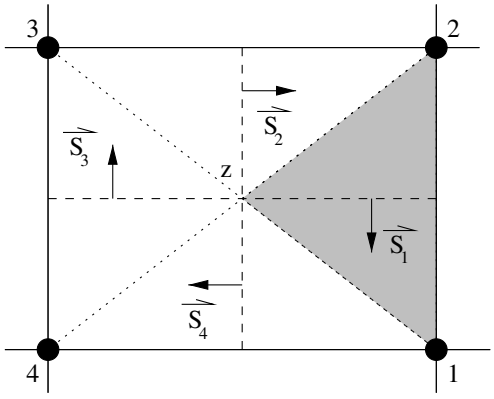

Fig. 1. Quadrilateral zone z: dotted interior lines delineate triangular subzones (gray), dashed lines form the median mesh with normal vectors $\vec{S}_1, \vec{S}_2, \vec{S}_3, \vec{S}_4$.

where the various terms are defined as follows: ρ_z and $c_{s,z}$ are the density and speed of sound in zone "z"; $\Delta\vec{v}_{21} \equiv \vec{v}_2 - \vec{v}_1$ is the difference in velocity along the edge "21" defined by points "1" and "2", from which are defined its magnitude $\Delta v_{21} \equiv |\Delta\vec{v}_{21}|$, and its direction $\widehat{\Delta v_{21}} \equiv \Delta\vec{v}_{21}/\Delta v_{21}$; the limiter function ψ_{21} is given in [1] and turns this force off for situations in which the velocity difference with respect to the edge direction is a linear function of the local coordinates; c_1 is a simple coefficient that is generally set to unity. This edge force is applied to points "1" and "2", with plus and minus signs, according to the compression switch $[\Delta\vec{v}_{21} \cdot \vec{S}_{21}]$; for the given definition of $\Delta\vec{v}_{21}$ and the orientation of the $\vec{S}_1$ vector in Fig. 1, compression is defined for $[\Delta\vec{v}_{21} \cdot \vec{S}_1] > 0$. Considering a frame of reference where $\vec{v}_1 = 0$, $\vec{f}_{21}^{\,\text{visc}}$ is then applied to point "1" with a "+" sign, and to point "2" with a "−" sign in order to ensure that this term acts in a dissipative manner [1]. If $[\Delta\vec{v}_{21} \cdot \vec{S}_1] < 0$, then $\vec{f}_{21}^{\,\text{visc}} = 0$. If the quantity in square brackets is summed over all edges of a zone and this sum is then divided by the zone volume, one obtains the negative divergence of the velocity field as defined by finite volume differencing: namely, $(\nabla \cdot \vec{v})_z = -\sum_e \Delta\vec{v}_e \cdot \vec{S}_e / V_z$, where "e" ranges over all edges of the given zone "z", and V_z is its volume. The work performed by Eq. (1.1), and all other forces in the discrete, compatible formulation of Lagrangian hydrodynamics, is given by the negative dot product of the particular force with the displacement in a timestep of the point that this force acts upon [2,3].

To correctly specify an effective sound speed with respect to the edge "21" for use in determining the CFL number for timestep determination, a sound speed "$c_{q,21}$" is defined by $c_{q,21}^2 \equiv c_1(1-\psi_{21})(c_{s,z}\Delta v_{21} + \Delta v_{21}^2)$; the effective edge sound speed is then defined as $\sqrt{c_{s,z}^2 + c_{q,21}^2}$. What has been done is to define an effective edge sound speed in the presence of dissipation that resembles the magnitude of the largest characteristic speed along an edge in 1D in the Lagrangian frame, which is $(c_{s,z} + \Delta v_{21})$. The CFL condition sets the timestep by requiring that this characteristic speed be resolved for all edges of all zones in the computational domain.

2. Curl-*q* force specification

The first attempt at turning Eq. (1.1) into a vorticity damping form of an artificial viscosity is to change the dot product in the compression switch into a cross product, obtaining $[\Delta\vec{v}_{21} \times \vec{S}_1]$. However, this quantity is a vector, and what is needed is an appropriate scalar. In order to construct a scalar the magnitude of $\Delta\vec{v}_{21}$ is separately factored out of this term and rewritten as a vector $l_{21,\perp}\vec{\omega}_z$, where $\vec{\omega}_z \equiv \sum_e \Delta\vec{v}_e \times \vec{S}_e / V_z$ is the finite volume difference form of the curl of the velocity field in zone "z", and $l_{21,\perp}$ is a length scale along edge "21" that is defined as $l_{21,\perp} \equiv |\widehat{\Delta v_{21}} \times \vec{l}_{21}|$; $\vec{l}_{21}$ is the vector distance between points "1" and "2" of edge "21". Now a dot product can be formed between $\vec{\omega}_z$ and the remaining factor, $(\widehat{\Delta v_{21}} \times \vec{S}_1)$, to obtain the desired scalar. Assembling these "postulates" results in our form for the "curl-q" force as

$$\vec{f}_{21}^{\,\text{curl-}q} = c_1(1-\psi_{21}^2)\rho_z(c_{s,z} + \Delta v_{21})[l_{21,\perp}\vec{\omega}_z \cdot (\widehat{\Delta v_{21}} \times \vec{S}_1)]\widehat{\Delta v_{21}}. \tag{2.1}$$

Note that this force is applied to grid points "1" and "2" with the same signs as that of the artificial viscosity force of Eq. (1.1). Also, if the term in square brackets is negative, $\vec{f}_{21}^{\text{curl-}q} = 0$, as required for it to act in a dissipative manner. Thus, all of the properties of the artificial viscosity that apply to Eq. (1.1), as enumerated in Ref. [1], are automatically transferred to the above definition of the curl-q force. In particular, this force turns off for rigid rotation due to the limiter function, and for grid-aligned flow because the lever arm $l_{21,\perp}$ is then zero. Because of this latter fact the limiter function has been weakened somewhat in Eq. (2.1) by using ψ_{21}^2 in place of ψ_{21} itself. This is a rather minor modification that allows us to run all test problems with the coefficient $c_1 = 1.0$ instead of somewhat larger values in certain cases. Also, to prevent numerical noise $l_{21,\perp}$ is set to zero if $l_{21,\perp}/|\vec{l}_{21}| < 10^{-3}$. Just as for the artificial viscosity force, the curl-q force contributes an effective sound speed along the given edge that is added to the sum of the squares of the zone sound speed and the artificial viscosity $c_{q,21}^2$ for timestep determination, as discussed previously. The square of the effective curl-q force sound speed is given simply by inspection of Eq. (2.1) as $c_1(1-\psi_{21}^2)(c_{s,z} + \Delta v_{21})l_{21,\perp}|\vec{\omega}_z|$.

The above form for the force is stated directly without reference to any term in a set of PDE's. That this is possible is a consequence of the discrete compatible form of Lagrangian hydrodynamics in that the discrete finite-volume description that it utilizes is more fundamental than the underlying continuum equations. For edge forces such as those given in Eqs. (1.1), (2.1), there exists no direct continuum limit, but only a loose analogy to terms in a differential equation. For the edge-centered artificial viscosity of Eq. (1.1), this analogy yields the term $q \equiv \rho(c_s + \Delta v)\Delta v$ in a zone "z", which in 1D allows one to insert $P \to P + q$ into all terms that contain the pressure "P". For the curl-q force of Eq. (2.2) such an analogy is more difficult to justify since $\vec{\omega}_z = 0$ in 1D, and this force vanishes. However, keeping this fact in mind one can still loosely make the analogy that the simple scalar form of the artificial viscosity ascribed above to Eq. (1.1) becomes

$$\rho_z(c_{s,z} + (\Delta v)_z)(\Delta v)_z \to \rho_z(c_{s,z} + |(\nabla \times \vec{v})_z| l_\perp) l_\perp |(\nabla \times \vec{v})_z|. \tag{2.2}$$

In this equation "$l_\perp$" is to be interpreted as some average length that is normal to Δv taken over all zone edges. Then this term augments the pressure "P", subject to the limiter and force on/off switch, as does the usual artificial viscosity.

3. Numerical results and discussion

Two well-known test problems are utilized to demonstrate the effectiveness of the new curl-q vorticity damping mechanism. These are Saltzman's piston [6], and Noh's problem [7], computed in both 2D and 3D Cartesian geometry. In the 2D case results of the curl-q force, in conjunction with the edge-centered artificial viscosity, are compared to a recently published "tensor" form of the artificial viscosity [4]. Unlike the edge-centered form, this tensor artificial viscosity contains zone information, and thus reduces the dependence of the solution on the relation of the grid to the flow direction. These test problems have a $\gamma = 5/3$ ideal gas law equation of state; they are run with all artificial viscosity coefficients, as well as "c_1" in Eq. (2.1), set to unity. Anti-hourglass subzone pressure forces as described in [8], with a "merit factor" of unity, are also utilized for all simulations. Modifications to the standard setups referenced above are indicated; comparisons in 2D are made within the same computer code [9].

We begin with the standard setup for the Saltzman piston problem in 2D Cartesian geometry that has been elongated by an amount of 3:1 in the shock wave (or driving piston, from left to right with unit velocity) direc-

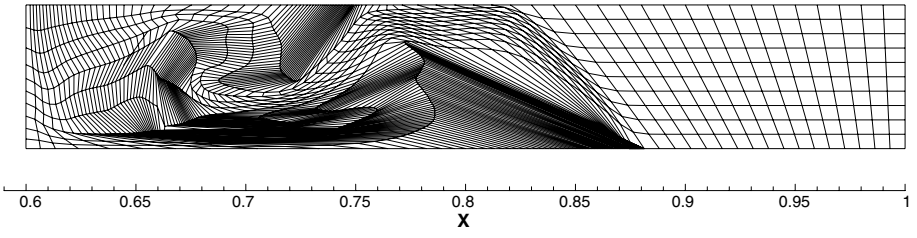

Fig. 2. Saltzmann piston in 2D – aspect ratio 3:1 – edge viscosity without curl damping, mesh at $t = 0.6$ before failure due to severe grid distorsion.

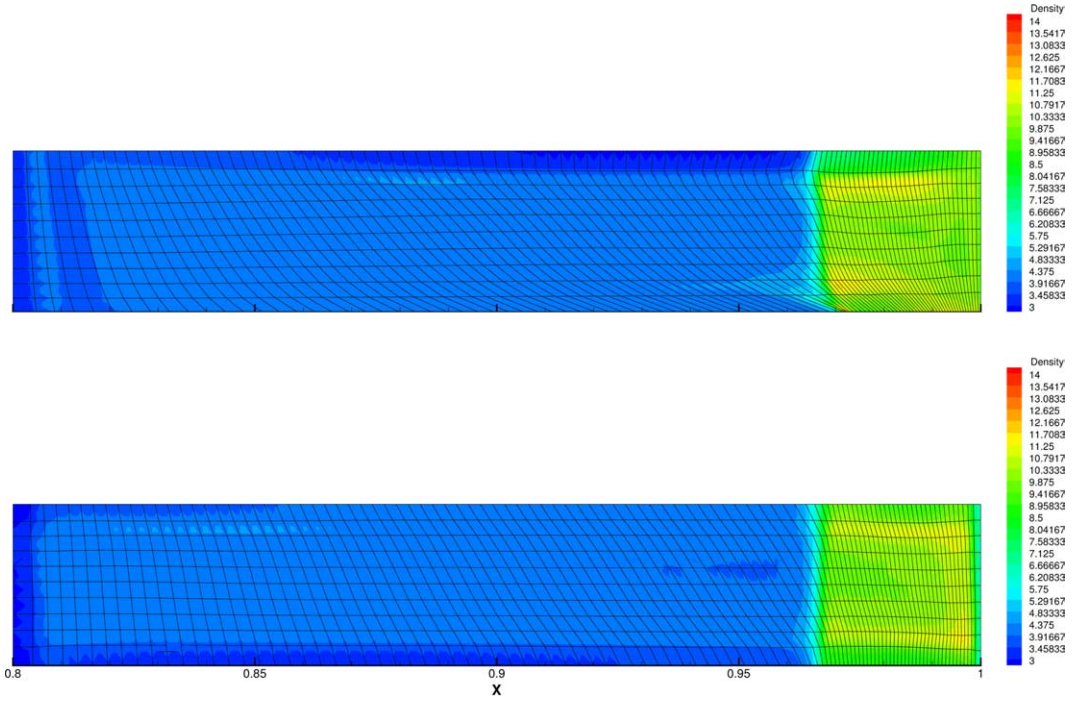

Fig. 3. Saltzmann piston in 2D – aspect ratio 3:1 – mesh and density. (Top) Edge viscosity with curl-q damping at $t = 0.8$. (Bottom) Tensor viscosity at $t = 0.8$.

tion. The result shown in Fig. 2 is the grid at time $t = 0.6$ without curl-q forces using the edge-centered artificial viscosity. The code fails due to severe grid distortion shortly after this time.

Results with the same initial and boundary conditions are given in the top and bottom parts of Fig. 3 at the final time of $t = 0.8$ for the edge-centered artificial viscosity with curl-q forces, and with the tensor artificial viscosity, respectively. At this time the shock wave has reflected from the fixed wall on the right side of the figure and is heading back towards the piston. Both of these cases show little grid distortion due to unphysical vorticity generation. These results show that the tensor artificial viscosity performs substantial damping of the unphysical vorticity that would otherwise be generated, and thus acts much like the curl-q damping force. If the grid is further elongated in the shock direction both the edge-centered artificial viscosity with curl-q force, and the tensor artificial viscosity, will fail; the former at about 4:1 aspect ratio, the latter at about 5:1. This is expected since as one further elongates the grid, pressure gradients in the ignorable vertical direction become larger, eventually leading to grid distortion and failure of the calculation. One can make modifications to increase the aspect ratio at which this failure occurs, but these can lead to non-positive heating of the artificial viscosity and curl-q forces that is unacceptable. Finally, if this problem is run with the grid highly elongated (10^4:1) in the ignorable, vertical direction as in [8], the net vorticity is small and the curl-q force has no discernable effect; in this case subzone, anti-hourglass forces are needed to obtain quality results.

Next, results are displayed for the Noh problem in 2D Cartesian geometry with initially square zones, 50×50, on a unit domain in both "x" and "y" directions. The initial velocity is minus one in the radial direction for all points, but zero at the $(0, 0)$ origin; a shock propagates outward from this point. Fig. 4 shows the grid and density at time $t = 0.6$ for three cases: part (a) gives the result for the edge-centered artificial viscosity without curl-q forces; part (b) is with curl-q forces added, and part (c) is with the tensor artificial viscosity alone. The latter two results are similiar, again showing that the tensor artificial viscosity damps unphysical vorticity much as the curl-q force does. The large jets seen in part (a) without curl-q damping can be thought of as arising from "false" vorticity present in the initial conditions using a square grid. The Noh problem is irrotational in its initial conditions, but on a square grid, and using our finite-volume formulas to compute the curl of the velocity field in the zone, one finds zero curl only on the 45° line; the curl of the velocity field

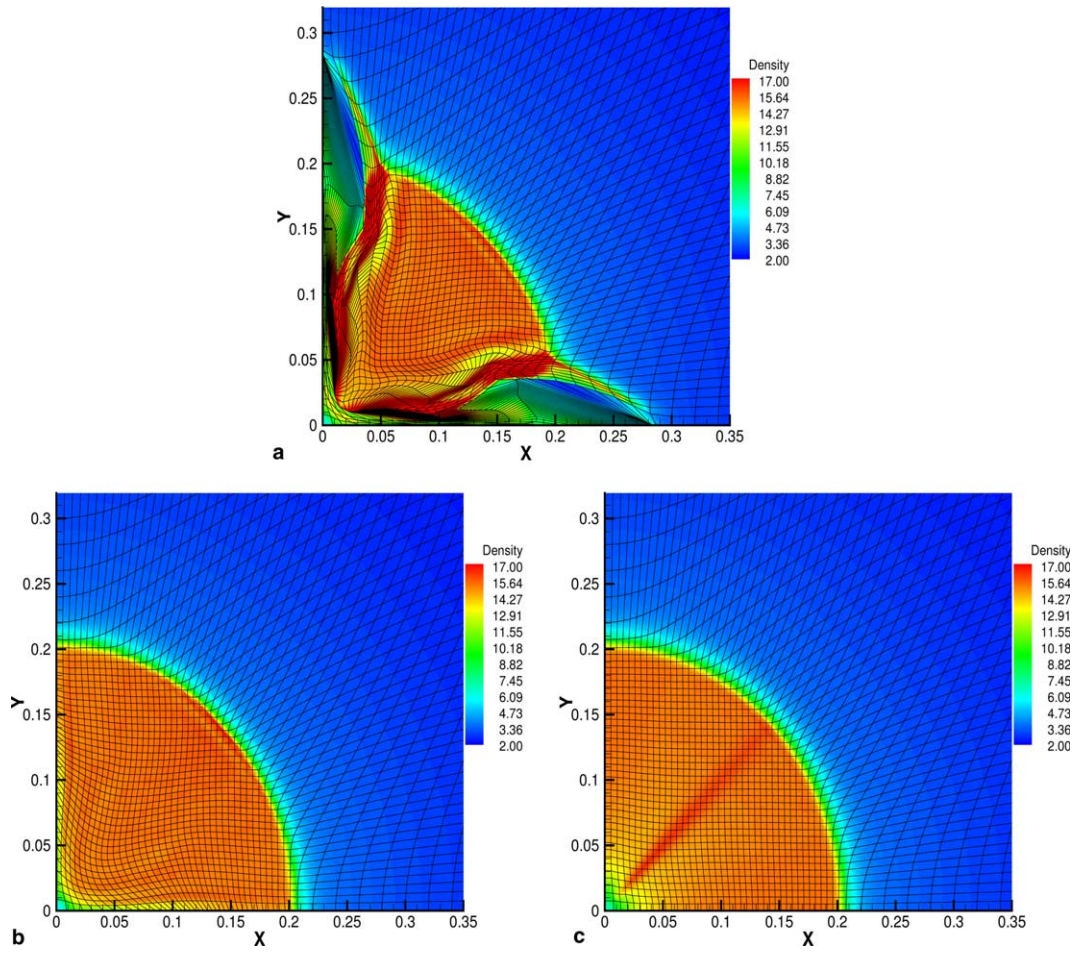

Fig. 4. Noh problem, 2D Cartesian geometry – mesh and density at time $t = 0.6$, the exact radius of the shock wave is $r = 0.2$. (a) Edge viscosity without curl damping, 1422 time steps. (b) Edge viscosity with curl damping, 606 time steps. (c) Tensor viscosity, 423 time steps.

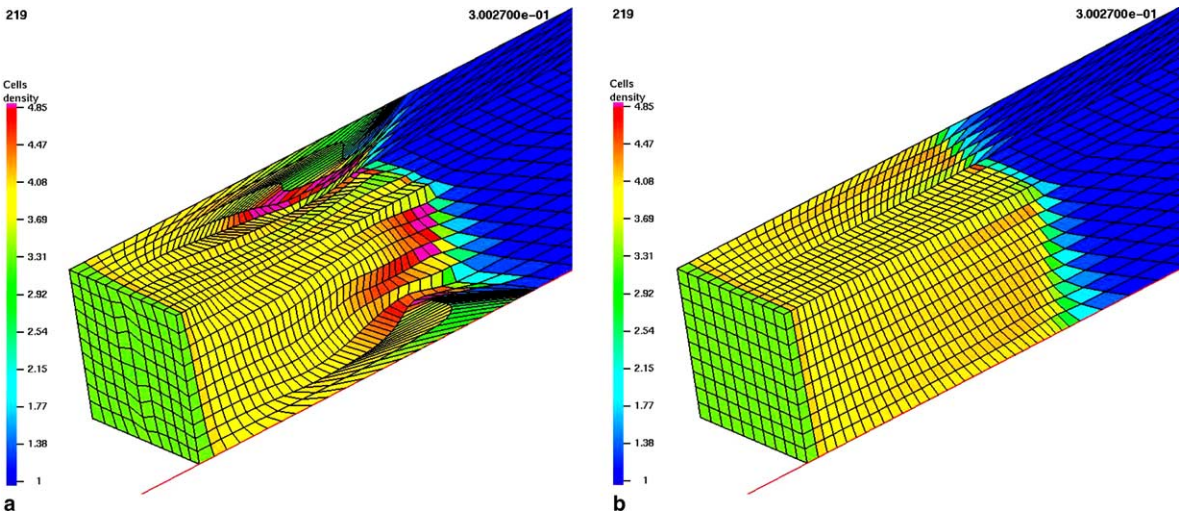

Fig. 5. Extended Saltzmann problem, 3D Cartesian geometry, aspect ratio 2:1 – edge viscosity – density and mesh at time $t \simeq 0.3$, density behind shock should be 4.0. (a) Without curl-q damping; fails due to mesh tangling soon after this time. (b) With curl-q damping; code runs to about $t = 0.7$ and then fails due to mesh tangling.

increases with magnitude and with opposite signs as one approaches the horizontal and vertical axes. The limiter functions keep the artificial viscosity and the curl-q force off until the shock wave propagates past any given point. Then, without the curl-q force or the tensor artificial viscosity, strong unphysical vorticity generation is seen to occur along the axes.

In 3D we show results with the extended version of the Saltzman piston problem as previously defined in [5]. This extended problem is completely 3D in its setup; the Saltzman skewing of the grid is made to change parity uniformly in the third dimension. This grid is compressed by a 2:1 aspect ratio in the non-shock directions so that zones are elongated by this amount in the shock direction. Fig. 5 shows the grid and density profile at time $t = 0.3$ for two cases: part (a) is without the curl-q force; this calculation fails shortly after this time due to unphysical grid distortion; part (b) is with the curl-q force at the same time and shows a quite satisfactory result. This latter simulation will fail later (at about $t = 0.7$) due to grid distortion about the vertical plane with the high (red) density spot seen in the top-middle of part (b) of this figure. Lagrangian codes can always be broken, and no amount of curl smoothing or other devices guarantees run to completion, much less correct answers.

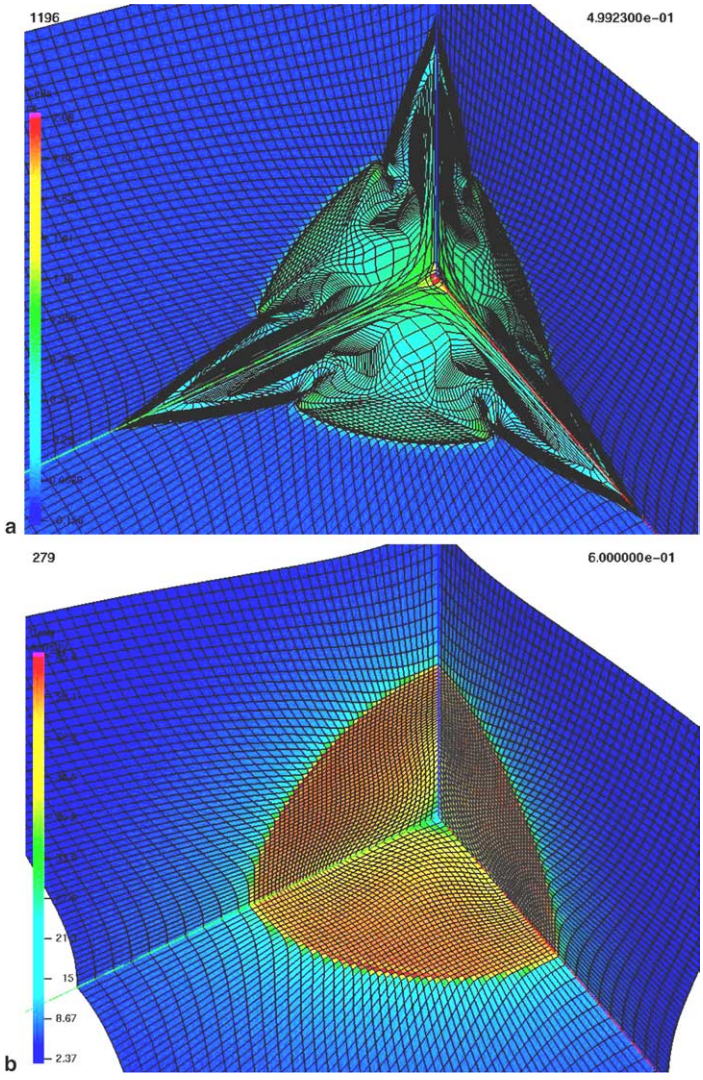

Fig. 6. Spherical Noh problem, 3D Cartesian geometry, one octant, 50^3 cubic initial grid – edge viscosity – corner is the origin. (a) Without curl-q damping, fails at time $t = 0.5$ due to mesh tangling at 1196 time steps. Specific internal energy is shown for contrast, density is unphysical due to the severe mesh distortion. (b) With curl-q damping at time $t = 0.6$, 279 time steps. Variable plotted is density, which matches the exact solution (shock wave at radius $r = 0.2$, density of 64, red color). Wall heating error is clearly visible.

Last, the Noh problem is calculated using initially cubic zones in 3D Cartesian geometry, $(50 \times 50 \times 50)$ for an octant. Fig. 6 has two parts: part (a) gives the grid at time $t = 0.5$ when the calculation fails due to excessive grid distortion without using any curl-q damping force. Jets along the three coordinate axes dominate the solution, which is colored using specific internal energy to obtain contrast; density has become unphysical due to zone collapse. Part (b) of this figure gives the result showing density at the final time $t = 0.6$ with curl-q forces. This latter result is of high quality for this problem; the ubiquitous wall-heating error is clearly visible, otherwise this is the correct solution for the 3D spherical Noh problem – a density of 64 behind the shock at a major radius of 0.2 at time $t = 0.6$.

In summary, the Lagrangian formulation of hydrodynamics produces reliable results only for irrotational, compressible, deterministic fluid flow. These conditions are strictly valid only in one-dimension. However, in multi-dimensions this may be the case to a substantial degree, particularly when the initial conditions of the simulation are homomorphic to one-dimensional geometry. Use of a vorticity damping mechanism as introduced herein is justified not only to remove unphysical vorticity, but also for calculations where physical vorticity is present but not dominant. In the latter case the solution may be incorrect in certain regions of the problem, but global, spatially integrated quantities may still remain substantially correct. If it is these quantities that are of principal interest, then Lagrangian frame calculations are appropriate. However, it is necessary to keep such calculations running to completion in order to assess these results. The "curl-q" term introduced herein affords a very simple and effective way to sustain Lagrangian calculations under such circumstances.

Acknowledgments

The authors acknowledge M. Shashkov for useful discussions. This work was supported by the Advanced Strategic Computing Initiative (ASCI) of the US Department of Energy.

References

[1] E.J. Caramana, M.J. Shashkov, P.P. Whalen, Formulations of artificial viscosity for multi-dimensional shock wave computations, J. Comp. Phys. 144 (1998) 70–97.
[2] E.J. Caramana, D.E. Burton, M.J. Shashkov, P.P. Whalen, The construction of compatible hydrodynamics algorithms utilizing conservation of total energy, J. Comp. Phys. 146 (1998) 227–262.
[3] R. Loubère, E.J. Caramana, The force/work differencing of exceptional points in the discrete, compatible formulation of Lagrangian hydrodynamics, LAUR-04-8906, J. Comp. Phys., accepted, doi:10.1016/j.jcp.2005.11.022.
[4] J.C. Campbell, M.J. Shashkov, A tensor artificial viscosity using a mimetic finite difference algorithm, J. Comp. Phys. 172 (2001) 739–765.
[5] E.J. Caramana, C.L. Rousculp, D.E. Burton, A compatible, energy and symmetry preserving Lagrangian hydrodynamics algorithm in three-dimensional cartesian geometry, J. Comp. Phys. 157 (2000) 89–119.
[6] J.K. Dukowicz, J.A. Meltz, Vorticity errors in multidimensional Lagrangian codes, J. Comp. Phys 99 (1992) 115–134.
[7] W.F. Noh, Errors for calculations of strong shocks using an artificial viscosity and an artificial heat flux, J. Comp. Phys. 72 (1987) 78.
[8] E.J. Caramana, M.J. Shashkov, Elimination of artificial grid distortion and hourglass-type motions by means of Lagrangian subzonal masses and pressures, J. Comp. Phys. 142 (1998) 521–561.
[9] R. Loubère, First steps into ALE. INC(ubator) A 2D ALE code on general code on general polygonal mesh for compressible flows – version 1.0.0, Los Alamos report, LAUR-04-8840.